Supporting Information

Trap remediation of $CuBi_2O_4$ nanopolyhedra via surface self-coordination by H_2O_2: An innovative signaling mode for cathodic photoelectrochemical bioassay

Mengmeng Gu,[a] Zhuying Yan,[b] Xiuming Wu,[a] Zaijun Li,[a] Yuming Dong,[a] Guang-Li Wang*[a,c]

[a]Key Laboratory of Synthetic and Biological Colloids (Ministry of Education), School of Chemical and Material Engineering, Jiangnan University, Wuxi 214122, China

[b]State Key Laboratory of Food Science and Technology, Jiangnan University, Wuxi, Jiangsu 214122, China

[c]Shandong Key Laboratory of Biochemical Analysis, College of Chemistry and Molecular Engineering, Qingdao University of Science and Technology, Qingdao 266042, China

*Corresponding author: Guang-Li Wang

*E-mail: glwang@jiangnan.edu.cn

Table of Contents

Materials. Bismuth nitrate ($Bi(NO_3)_3 \cdot 5H_2O$) and copper nitrate ($Cu(NO_3)_2 \cdot 3H_2O$) were purchased from Sigma-Aldrich Corporation (St. Louis, MO, USA). The Flap endonuclease 1 (FEN1) was obtained from PXN Biotechnology Co., Ltd. (Tianjin, China). The single-walled carbon nanotubes (SWCNT) were acquired from Nanotech Port Co., Ltd. (Shenzhen, China). Glioma samples were taken from Wuxi Hospital of Traditional Chinese Medicine (Wuxi, China). HeLa cells were purchased from the American Type Culture Collection (Manassas, USA). The FEN1 enzyme linked immunosorbent assay (ELISA) kits were supplied by Jianglai Biotechnology Co., Ltd. (Shanghai, China). Concentrated nitric acid (HNO_3), ethylene glycol (EG), sodium hydroxide (NaOH), and hydrogen peroxide (H_2O_2, 30%) were all acquired from Sinopharm Chemical Reagent Co., Ltd. (Shanghai, China). The nucleoprotein extraction kits and all oligonucleotides (HPLC-purified) were purchased from Sangon Biotechnology Co., Ltd. (Shanghai, China), and the corresponding oligonucleotide sequences are provided in Table S1.

Table S1. Oligonucleotide sequences employed in this work

Name	Sequence (5′ to 3′)
P1	ATG ATA CCG CCG AGA AGA GCA CAT CGT TCG ACA TTA CAA AGT CTG AAT CCT TAC A
P2	CAT AAC CTG GGA GCG TAG ATA ATG TCG AAC GAT GTG ACA GTT GAC GGA CCA CTA T
P3	TAC GCT CCC AGG TTA TGT TTG CTG TGA TGC ACC CTT CGT GTA AGG ATT CAG ACT T
P4	CTC TAA CTT TAA TTC TCA GCT AAC TTT TGA TTT TTC TTC TCG GCG GTA TCA TCT AAG GGT GCA TCA CAG CAA AAT AGT GGT CCG TCA ACT
P5	AAT GTT CAG TGA GCG AGA ATT AAA GTT AGA G
P6	TCA AAA GTT AGC TA
P7	TTC AGT GAG CTT TTT CTT CTC GGC GGT ATC ATC TAA GGG TGC ATC ACA GCA AAA TAG TGG TCC GTC AAC T
P8	CAT CCC GCC CAA CCC GCT CAC TGA ACA TT
P9	AAT GTT CAG TGA GCG GGT TGG GCG GGA TGG GTT TTT CTT CTC GGC GGT ATC ATC TAA GGG TGC ATC ACA GCA AAA TAG TGG TCC GTC AAC T

Apparatus. Scanning electron microscopy (SEM) images were obtained from a Hitachi S-4800

high resolution scanning electron microscope (Hitachi, Japan). The X-ray diffraction (XRD) pattern was observed with an X'Pert Philips materials research diffractometer (Bruker AXS, Germany). The X-ray photoelectron spectroscopy (XPS) was acquired from an Axis supra spectrometer (Kratos, UK). The Raman spectra were retrieved from an InVia Raman microscope spectrometer (Renishaw, UK). The photocurrent measurements, electrochemical impedance spectroscopy (EIS), and current−voltage (J−V) curves were conducted on a CHI 800C electrochemical workstation (Shanghai, China). The thermally stimulated current (TSC) assays were conducted on a Concept 40 broadband impedance spectrometer (Novocontrol, Germany). The photoluminescence (PL) spectra were performed on an FS5 fluorescence spectrometer (Edinburgh, UK). Fluorescence lifetimes were acquired from a Lifespec II time-resolved fluorescence lifetime spectrometer (Edinburgh, UK). The surface photovoltage (SPV) spectroscopy was obtained from a PL-SPS1000 surface photovoltage spectrometer (Zolix, China). The UV-vis diffuse reflectance spectra (UV-vis DRS) were acquired from an UV-vis-NIR-3600 spectrophotometer (Shimadzu, Japan). The atomic force microscopy (AFM) was conducted on a Multimode 8 atomic force microscope (Bruker, Germany). Transmission electron microscopy (TEM) images were acquired from a JEM-2100 Plus transmission electron microscope (Hitachi, Japan). The dynamic light scattering (DLS) assays were performed with a ZetaPALS analyzer (Bruker, USA). The circular dichroism (CD) experiments were conducted on a Chirascan V100 spectropolarimeter (Applied Photophysics Ltd., UK).

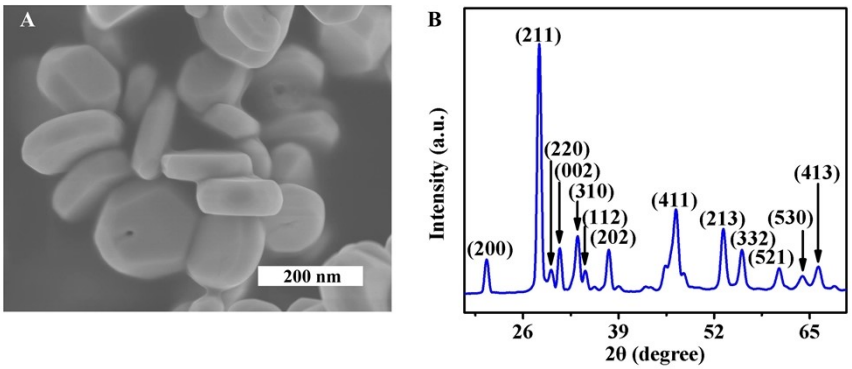

Fig. S1 (A) SEM image and (B) XRD pattern of the as-prepared $CuBi_2O_4$ nanopolyhedra.

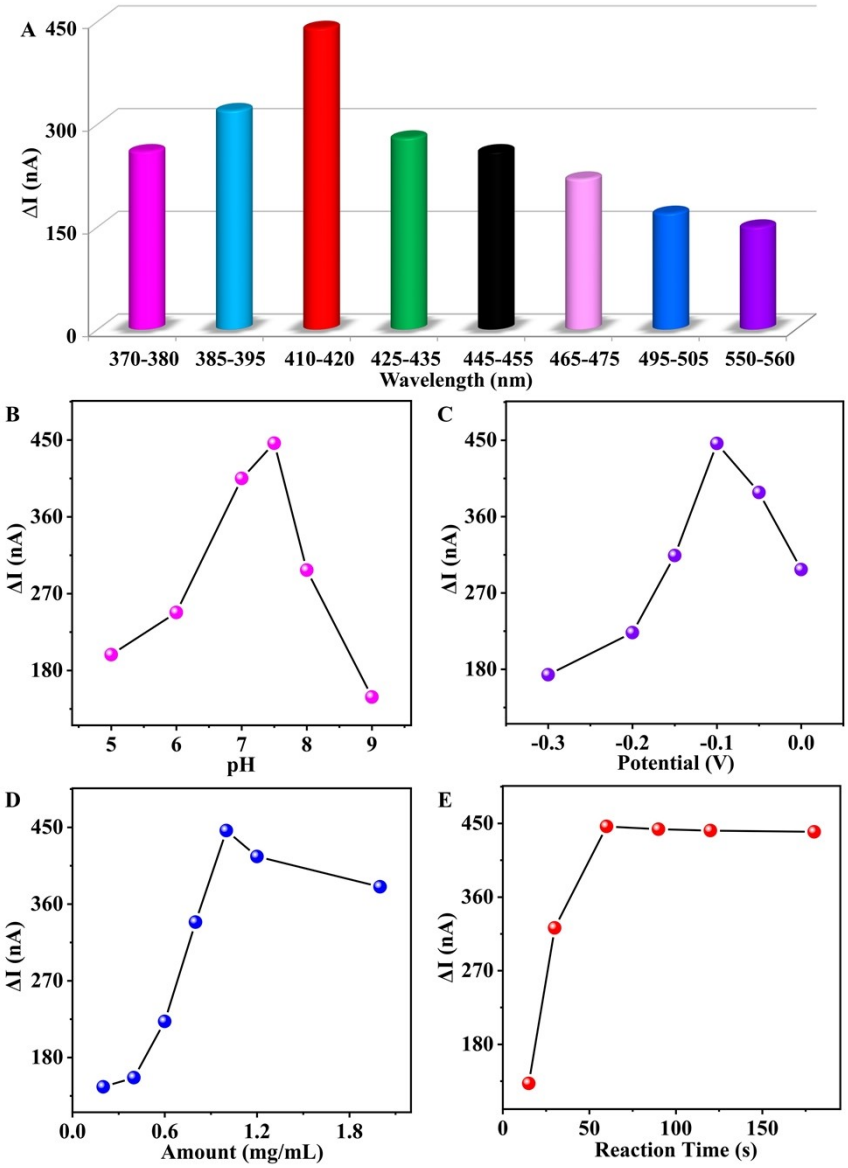

Fig. S2 Influence of (A) excitation wavelength, (B) testing electrolyte pH, (C) applied potential, (D) amount of $CuBi_2O_4$ dropped, and (E) reaction time on the PEC signal increment of the $CuBi_2O_4$ modified electrode to H_2O_2 (10 mM).

As illustrated in Fig. S2, we explored the effects of different conditions (including the light irradiation wavelength, PEC testing electrolyte pH, applied potential, $CuBi_2O_4$ material dosage deposited, and the reaction time of $CuBi_2O_4$ electrode with H_2O_2) on the photocurrent responses of the $CuBi_2O_4$ modified electrode to H_2O_2. And the corresponding optimal conditions were obtained as 460~470 nm, pH 7.4, –0.1 V (*vs*. saturated Ag/AgCl), 1.0 mg/mL, and 60 s, respectively. Under the desired reaction conditions described above, the intensity of the photocurrents enhanced with the increase of H_2O_2 concentrations (Fig. S3A), and the increment (ΔI) of the PEC signal was linear with the logarithm of the concentration of H_2O_2 in the range of 0.7 μM–10 mM (Fig. S3B). The detection limit was calculated to be 0.23 μM (S/N=3).

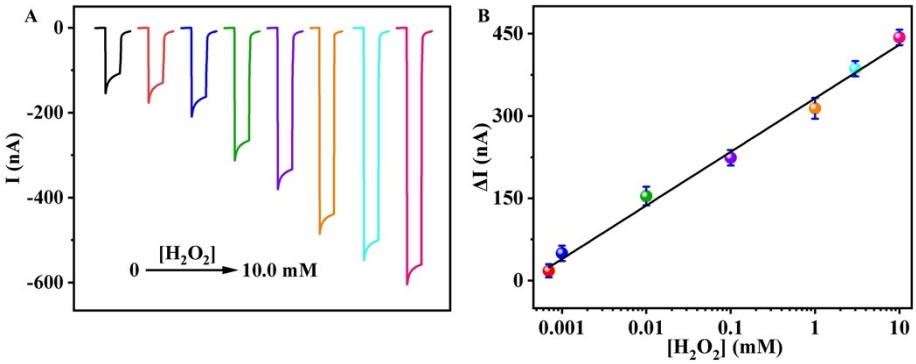

Fig. S3 (A) Photocurrent responses of $CuBi_2O_4$ modified ITO electrode to different concentrations of H_2O_2 (the concentration of H_2O_2 from left to right is 0, 0.0007, 0.001, 0.01, 0.1, 1.0, 3.0, and 10.0 mM, respectively). (B) The corresponding calibration curve.

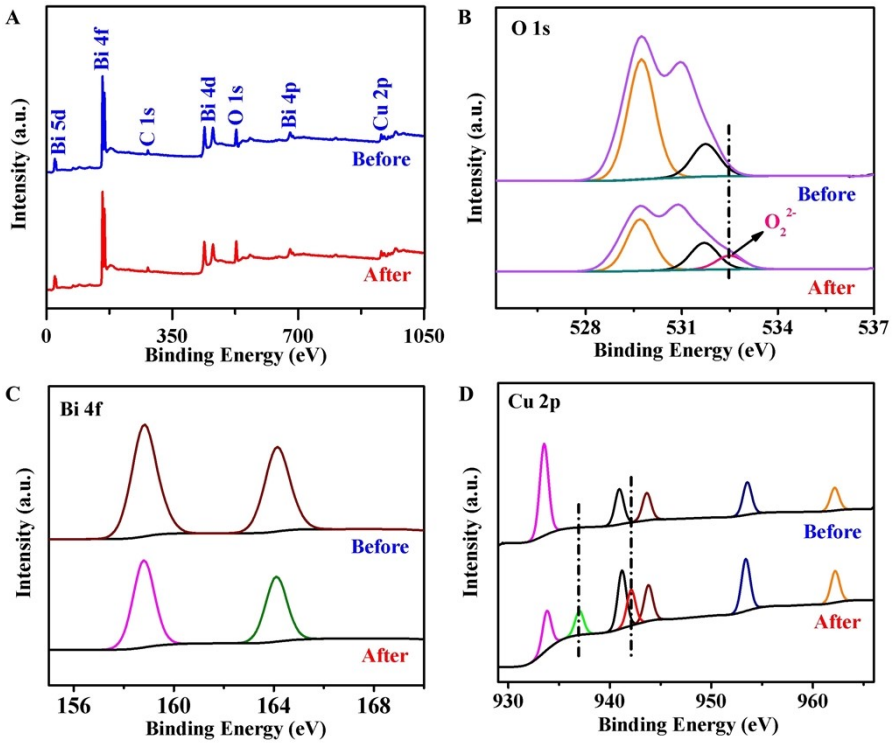

Fig. S4 (A) XPS survey spectra of $CuBi_2O_4$ before and after reaction with H_2O_2. High-resolution XPS spectra of (B) O 1s, (C) Bi 4f, and (D) Cu 2p.

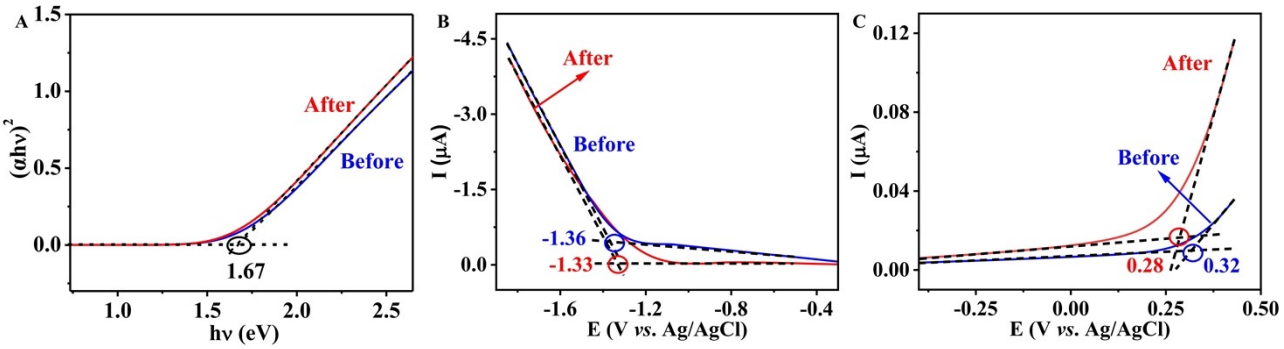

Fig. S5 (A) The Tauc plots of $(\alpha h\nu)^2$ versus photon energy ($h\nu$), and the LSV curve for measuring the (B) CB and (C) VB edges of $CuBi_2O_4$ before and after reaction with H_2O_2.

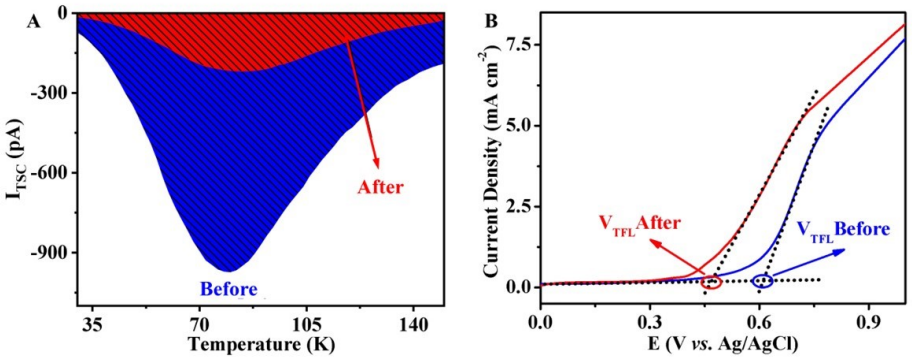

Fig. S6 (A) TSC spectra of $CuBi_2O_4$ before and after reacted with H_2O_2. Test conditions for TSC: The polarization temperature is 60 °C, the polarization time is 10 min, and the applied field strength is 600 V/min. (B) J−V curves of $CuBi_2O_4$ electrode before and after reacted with H_2O_2 under illumination with LED light source in the 410~420 nm band.

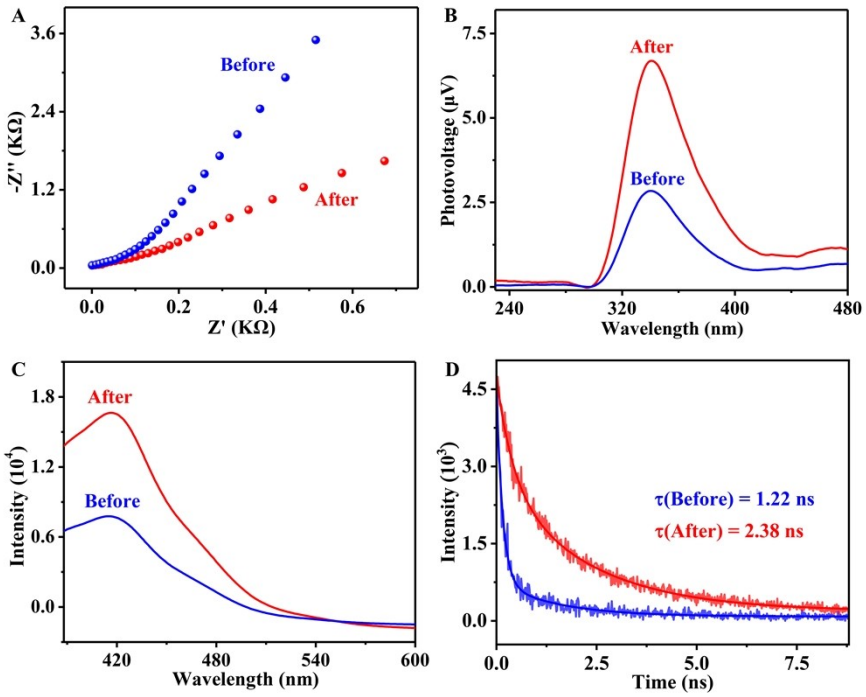

Fig. S7 (A) Nyquist impedance plots, (B) SPV spectroscopy, (C) PL spectra, and (D) TRPL spectra of $CuBi_2O_4$ before and after reacted with H_2O_2.

Table S2. Summary of the decay lifetimes of $CuBi_2O_4$ before and after reaction with H_2O_2

Sample	A_1	τ_1 (ns)	A_2	τ_2 (ns)	χ^2	τ_{avg} (ns)
$CuBi_2O_4$	384.60	0.18	67.25	1.81	0.98	1.22
$CuBi_2O_4/H_2O_2$	194.75	0.49	260.31	2.64	0.99	2.38

Note: The fitting model is $Y = A_1 e^{-\frac{X}{\tau_1}} + A_2 e^{-\frac{X}{\tau_2}}$, $\tau_{avg} = \frac{A_1\tau_1^2 + A_2\tau_2^2}{A_1\tau_1 + A_2\tau_2}$, where A_1 and A_2 indicate the decay constants, τ_1 and τ_2 represent decay times.

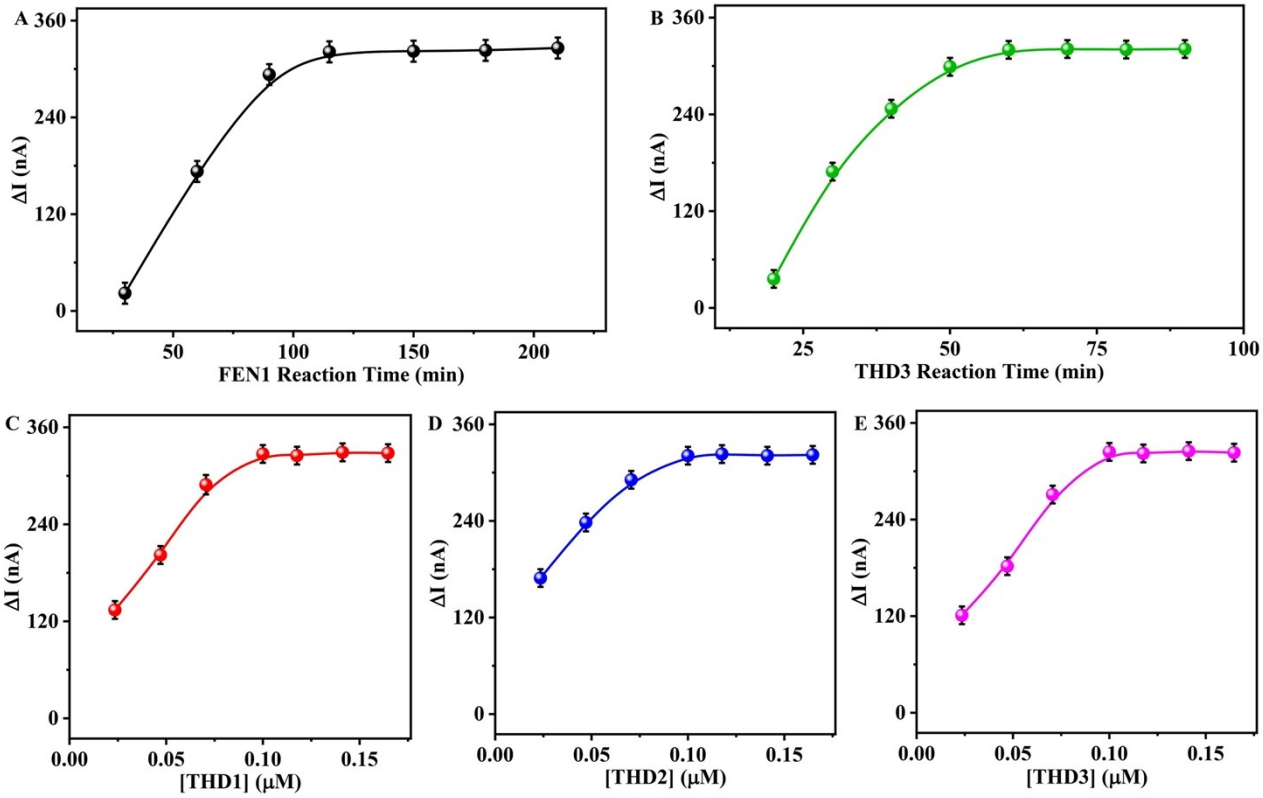

Fig. S8 Optimization of (A) incubation time of FEN1, (B) reaction time for G-quadruplex formation by THD3 rich in G bases, the concentration of (C) THD1, (D) THD2, and (E) THD3 for PEC detection of FEN1.

As shown in Fig. S8, when the incubation time of FEN1 was 115 min, the reaction time for G-quadruplex formation by THD3 rich in G bases was 60 min, and the concentration of THD1, THD2, and THD3 were all at 0.1 μM respectively, the photocurrent intensity reached maxima, suggesting that the above results were ideal reaction conditions. Under optimal conditions, the PEC assay was executed for the quantitative analysis of FEN1.

Table S3. Comparison with other reported methods for the analysis of FEN1

Method	Material	Linear Range (pM)	LOD (fM)	Reference
RT-PCR	——	semiquantitative	——	1
Western blot	——	qualitative	——	2
Immunohistochemistry	——	qualitative	——	3
Fluorometry	GO	0.2−100.0	380.0	4
Fluorometry	——	0.001−10.0	0.5	5
Fluorometry	——	0.02−8.0	15.0	6
Photoelectrochemistry	$CuBi_2O_4$	0.001−100.0	0.3	This work

Table S4. Recovery assay of FEN1 by spiking into real samples extracted from glioma and HeLa cells

Sample	Content (pM)	Spiked (pM)	Found (pM)	Recovery (%)	RSD (n=5, %)
Glioma	2.8	1.0	3.9	110.0	1.7
		5.0	7.8	100.0	1.9
		10.0	13.1	103.0	2.1
HeLa cells	3.6	1.0	4.7	110.0	1.8
		5.0	8.7	102.0	2.0
		10.0	13.5	99.0	1.8

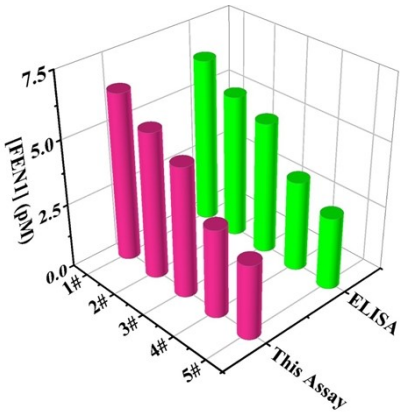

Fig. S9 FEN1 analysis in glioma samples was performed exploiting our PEC method and ELISA method.

Table S5. The correlations between our PEC method and ELISA method for the quantification of FEN1 in glioma samples

Sample (#)	This Assay (pM)	ELISA Method (pM)	Relative Error (%)
1	6.47	6.38	+1.41
2	5.63	5.54	+1.62
3	5.02	5.11	-1.76
4	3.41	3.50	-2.57
5	2.87	2.81	+2.14

References

[1] K. Wang, C. Xie and D. Chen, *Int. J. Mol. Med*., 2014, **33**, 1268−1274.

[2] T. Nikolova, M. Christmann and B. Kaina, *Anticancer Res*., 2009, **29**, 2453−2459.

[3] L. He, Y. Zhang, H. Sun, F. Jiang, H. Yang, H. Wu, T. Zhou, S. Hu, C. S. Kathera, X. Wang, H. Chen, H. Li, B. Shen, Y. Zhu and Z. Guo, *EBioMedicine*, 2016, **14**, 32−43.

[4] H. Zhang, S. Ba, D. Mahajan, J. Y. Lee, R. J. Ye, F. W. Shao, L. Lu and T. H. Li, *Nano Lett*., 2018, **18**, 7383−7388.

[5] B. Zhou, L. Lin and B. Z. Li, *Sens. Actuat. B: Chem*., 2021, **346**, 130457.

[6] B. Z. Li, A. Q. Xia, S. Y. Xie, L. Lin, Z. R. Ji, T. Y. Suo, X. Zhang and H. Huang, *Anal. Chem*., 2021, **93**, 3287−3294.